COSPAR Paper STP.I.2.5

GLOBAL SOLAR MAGNETIC FIELDS

J. Todd Hoeksema

Center for Space Science and Astrophysics, Stanford University, E.R.L. 322
Stanford, CA 94305-4055 U.S.A.

*To be published in the Journal of Geomagnetism and Geoelectricity, **43**, 1991.*

bstract

The global solar magnetic field greatly affects the corona, heliosphere, and terrestrial environment as well as revealing much about the Sun itself. It may be useful to think of the global field in two ways: as an aggregate of many small scale processes and as an entity.

When considering the origin and evolution of the global field, one immediately focuses on the smaller-scale features and processes that it comprises. These include the emergence of active regions, the interaction of new and existing flux patterns, the distortion and dispersal of flux over the surface by convective motions, the phenomena that produce the emergence of patterns with various periods, and the influence of convection and rotation at various depths on flux tubes.

When contemplating the effects of the global field, one often focuses on it as an entity or on its large-scale features. Examples are the reversal of the polar fields, the asymmetry between the north and south hemispheres, the dipole or quadrupole structure of the coronal field and its observation at the Earth as 2 or 4 polarity sectors, and the rigid rotation seen in coronal holes. Both views help us appreciate the significance of the global field.

Introduction

The global magnetic field of the Sun is made up of smaller-scale elements. These small features form patterns on the large scale that change relatively slowly. The large-scale organization is important for what it reveals about the internal processes of circulation and about field organization and production, as well as for its influence on the corona and interplanetary medium and, therefore, on the Earth.

It now seems that the large-scale field pattern can be largely explained in terms of the small intense field elements emerging in active regions and the relatively well understood effects of diffusion, differential rotation, and large-scale flows that act to disperse, transport, and cancel them. Therefore understanding the global field ultimately requires a knowledge of the origin of the small-scale elements composing it. That knowledge is not yet available.

However, to aid in the search for understanding the source of the magnetic field , it is helpful to know all of the characteristics of the field that must be explained. In this paper we concentrate on some of the large-scale features of solar magnetism that may offer clues to understanding the solar cycle: the polar magnetic field, the zonal magnetic field, and the rotation of the large-scale field pattern. While we try to relate these characteristics to their small-scale sources, we cannot yet explain why the small-scale features appear where and when they do.

The Polar Magnetic Field

The most stable large-scale magnetic regions are the polar fields. The polar fields reverse polarity at, or a little later than, solar maximum, and gradually increase in strength until the following minimum. The two hemispheres do not necessarily reverse polarity at the same time. The lower panel of Figure 1 shows the evolution of the northern and southern magnetic field strengths from the minimum of Cycle 21 to the maximum of Cycle 22, from mid-1976 to mid-1990. The polar field was positive in the north in 1976. The lighter, more variable lines show the line-of-sight magnetic field strength averaged over 30 days, as measured in the polemost apertures of the Wilcox Solar Observatory (WSO) magnetograms.

WSO uses a Babcock magnetograph to make daily 3 arc-minute observations of the Sun with high precision and a low zero level error (Scherrer et al., 1977, Duvall, 1977). 3 arc minutes is about one tenth of the solar diameter. Consequently, the polemost aperture extends from 55° latitude to the poles, and observations of the area within the polemost apertures reflect the polar field strength over a large area. Because the fields in the photosphere are approximately radial, the line-of-sight measurement is only a small fraction of the true field. Even so, the annual variation of the field strength due to the 7.25° inclination of the Earth's orbit makes it possible to estimate how the polar fields are distributed (Svalgaard et al., 1978; Hoeksema, 1984). The field is strongest in the north in early September, when that pole is tipped toward the Earth. The field values in the figure are corrected for neither the line-of-sight projection nor the known saturation of the field measurements made with the 5250Å spectral line.

The smoother, heavier lines show the field strength smoothed with a 20 nhz filter that removes any variations with periods less than about 1.5 years. The annual variations about this curve are large near solar minimum; just after solar maximum they are quite small. The variation cannot be explained by a relatively smooth dipole field distribution at solar minimum. To produce the observed annual signal requires a strong radial field, sharply peaked toward the pole. Svalgaard et al. (1978) found that the observed variation in 1976-1977 was best explained by a $11.5 \cos^8\Theta$ radial field distribution (corrected for saturation and projection). The average field strength in the polar cap was about half that value. The values were comparable in the two hemispheres and in adjacent polar apertures. During the more recent solar minimum, the observed field values were about 25% greater in each hemisphere, and the annual variations were comparable to those observed in 1977.

The two polar caps are similar in behavior, but not identical. Particularly in the most recent minimum, the southern field strength was greater than the north. That is perhaps most easily seen in the upper panel of Figure 1. The thin solid line shows the northern field strength: the dotted line shows the negative of the field strength at the southern pole. The slightly thicker, less variable solid line shows the average of the two, and the thickest smooth line shows the filtered average field strength. The fact that there is little annual variation in the average field strength indicates that the sharply-peaked part of the polar field is roughly symmetric, even though the average

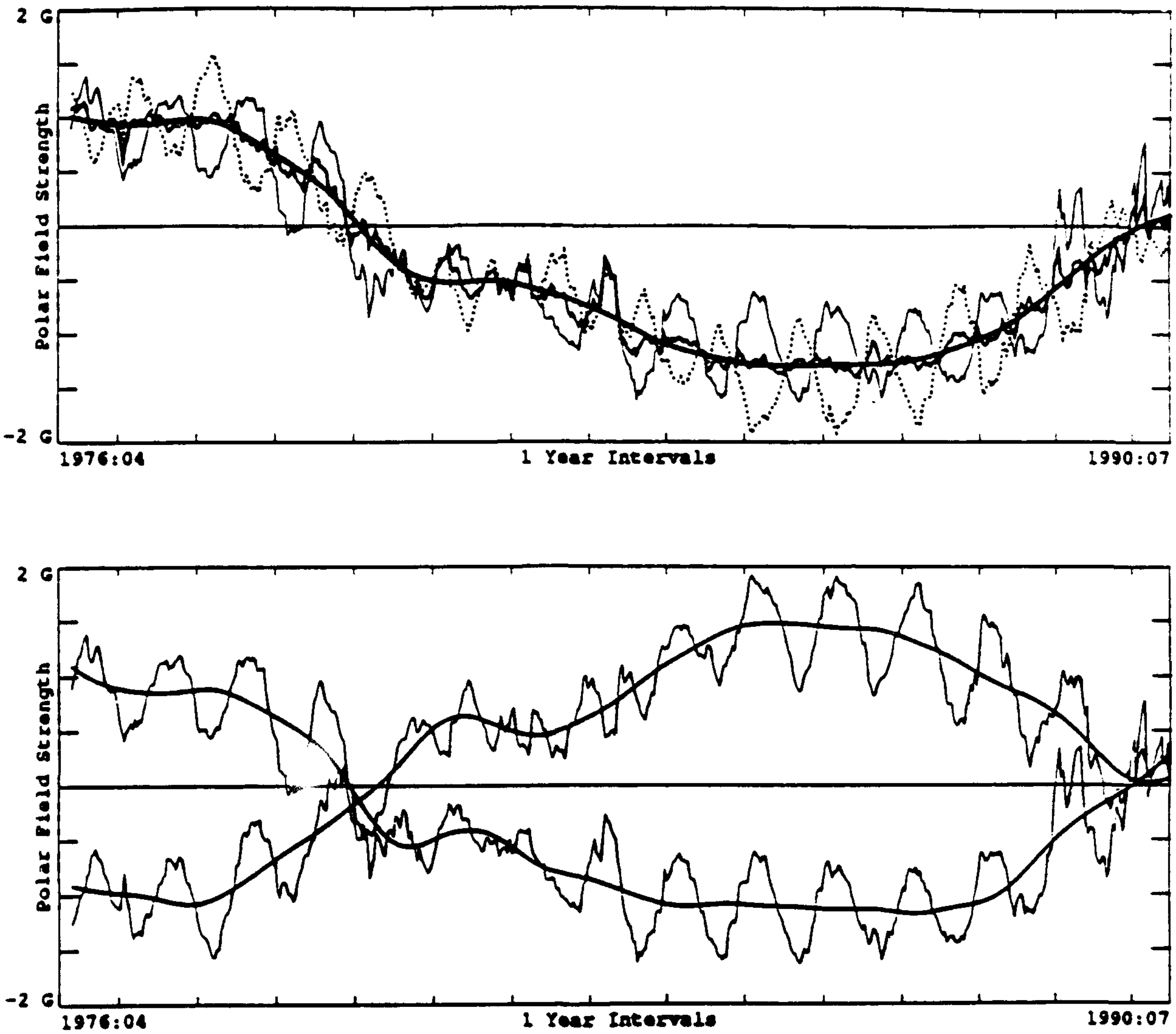

Figure 1: The lower panel shows the polar field strength measured at the Wilcox Solar Observatory from May, 1976 to July, 1990. The northern field was positive in 1976; it reversed polarity in 1980 and again at the beginning of 1990. The points are 30-day averages of the polemost 3 arc minute aperture of WSO daily magnetograms. The observations are not corrected for line-of-sight projection or for magnetograph saturation. The smooth curves are filtered to include signals with frequencies less than 20 nHz (1.6 years). The annual oscillations are caused by the changing projection of the strongly peaked polar fields due to the 7.25° inclination of the Earth's orbit. The north pole is seen more directly in September. The southern field is stronger than the northern field in 1986. The polar fields are about 25% stronger at solar minimum in 1986 than at minimum in 1976. The polar fields reverse at different times and with differing stability. The upper panel shows the northern and the negative of the southern field as the thinner solid and dotted lines, respectively. The less variable heavier line is the average of the two. The degree to which there is no annual period indicates that the peaked fields are fairly symmetric. The heavy smooth curve shows the 20 nHz low pass average field strength.

values are different. The times of greatest variation in the average field will be discussed below.

In addition to the difference in strength, the two hemispheres reverse polarity at slightly different times. This is apparent in the smoothed averages in 1979 and, tentatively, in 1990. Past polar field reversals have often been more definite in one hemisphere than the other (Babcock, 1959; Howard and LaBonte, 1981). Close inspection of the lower panel shows that the southern field in the range from 55° to the pole appeared to reverse twice - in mid 1979 and again in 1980. The northern field reversed earlier and more definitely, although some of the difference may have to do with the coincidence of the reversal time with the Earth's annual north-south motion. It must be remembered that these coarse resolution data are different than other higher-resolution measurements.

Finer spatial scale observations give a consistent but somewhat complementary picture of what is happening at the poles. Tang and Wang (1990) have analyzed 1 arc-second polar data from the video magnetograph at Big Bear Solar Observatory (BBSO) recorded on 57 days since 1986. They find that the polar reversal begins at lower latitudes and gradually progresses toward the poles. Comparison of equatorial and polar limb measurements shows that the mean flux density at the poles at solar maximum resembles the quiet sun, but at solar minimum it is a little greater than quiet sun. The polarity distribution, of course, is different. The results are in general agreement with the field magnitudes observed at WSO, with average field magnitudes of about 1 Gauss near solar minimum and near zero at solar maximum. Unfortunately, the observations are infrequent and appear to have a greater zero level error. The southern fields are stronger than the northern fields from 1986 to 1988. A large annual variation in mean flux density is observed between 70° and the south pole in 1989 – from about 20 Gauss (corrected for limb darkening and projection, assuming a radial field) in February when the south pole is tipped toward the Earth, to about 8 Gauss in September when it is tipped away. This variation corresponds fairly well to the 1 G to 0 G variation seen in the line-of-sight southern field at WSO in 1989 between 55° and the pole. This suggests that even in 1989, when the polar field was decaying, a strongly peaked field existed (though over only a narrow latitude range). Note that some of the variation is likely due to the decay of the polar field over the six-month interval.

The conclusion is that the low and high resolution observations are consistent, subject to the inherent limitations of each measurement. The low resolution observations measure the net flux accurately with a low zero level error, but are unable to directly resolve the peaked field and are subject to additional uncertainties due to limb effects. The high resolution observations have relatively good accuracy in the mean flux density and in localizing flux changes, but the zero level noise is critical for determining the polarity.

Where does the polar field come from? It is generally agreed that the polar field arises from the remains of decaying active regions. In an ongoing series of simulations of the solar magnetic field, DeVore and Sheeley (1987) showed that the polar field can be calculated using only the measured flux emerging in active regions, the diffusion of flux elements, differential rotation, and a small meridional flow to reproduce the observations. When the model parameters are tuned to most accurately predict the lower-latitude field patterns, the calculated polar cap field distribution matches quite well the strong, sharply peaked field derived to explain the annual variation in WSO observations (Sheeley, Wang, and DeVore, 1989). While not without controversy (see discussion of rotation below), these empirical model results lend some support to this interpretation of the polar field measurements.

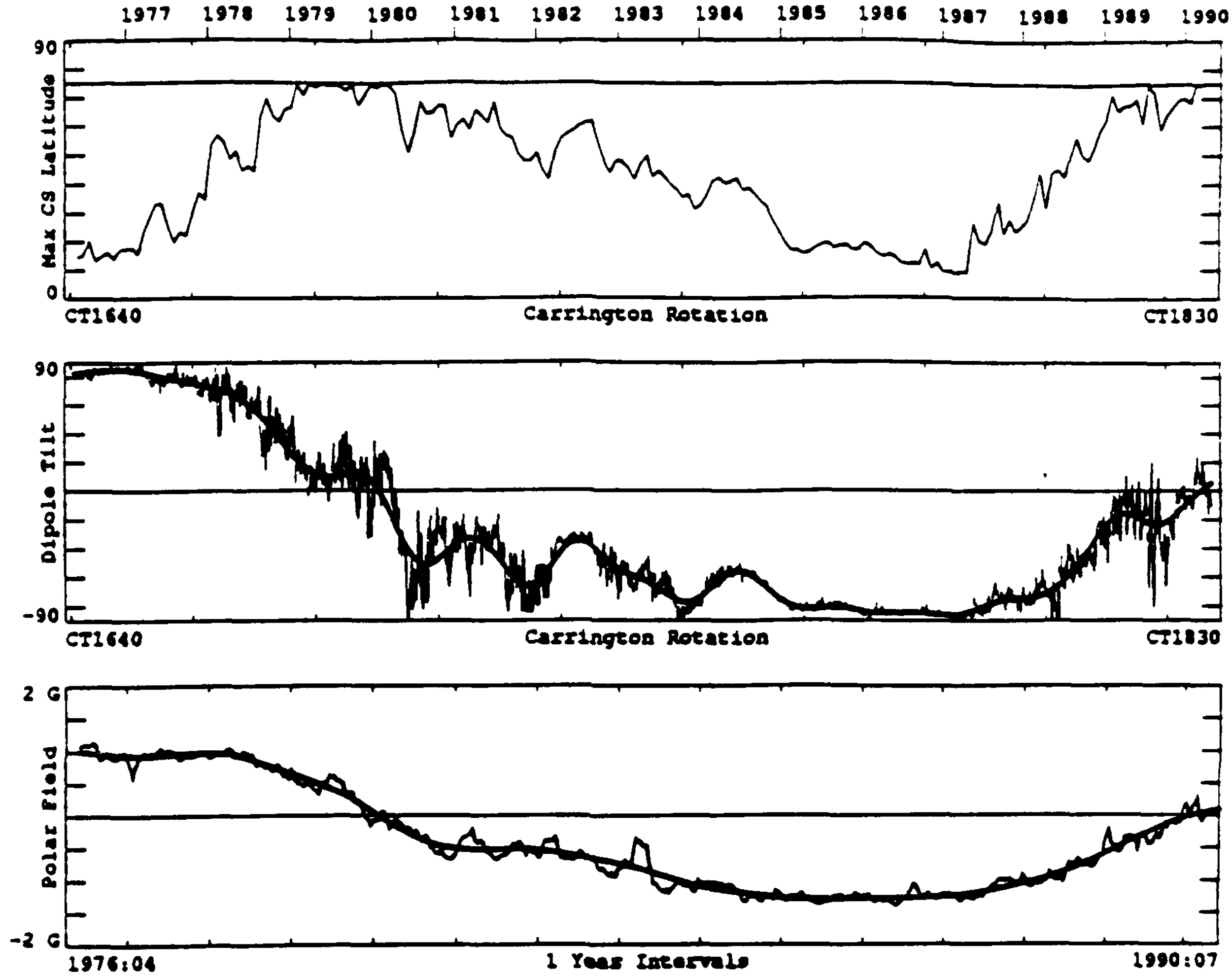

Figure 2: The lower panel shows the polar field strength described in Figure 1. The smooth curve is the filtered version of the average field strength measured in the northern and southern hemispheres. The center panel shows the tilt angle of the total dipole field calculated from the global photospheric field observations. Individual points are calculated each 10° of Carrington longitude and are affected by evolution of active regions. The smoothed curve is a 1-year low-pass filter of the dipole angle. The photospheric observations for this and the upper panel have been corrected to include the sharply peaked field derived from the annual observations, as discussed in the text. The top panel shows the maximum extent in latitude of the heliospheric current sheet. The coronal field determines the configuration of the interplanetary medium and is calculated using a potential field model and the photospheric field observations. There is an artificial maximum latitudinal extent of 70° because of the poor resolution of the polar field measurements. The latitudinal extent of the current sheet is a minimum when the polar field strength is a maximum. The current sheet was flatter in 1986 than in 1976.

The model says nothing about why the fields erupt to the surface as they do. There are some correlations between the polar field strength at minimum and the characteristics of the following cycle, e.g. Öhl's law. However, if the polar field is just leftover flux from the previous activity cycle that remains at the poles until destroyed by the next cycle's decaying active region flux, there is no reason to believe the polar fields are anything more than surface fields that do not interact with the fields in the interior that drive the solar cycle.

The polar field is related to other aspects of the global field. Figure 2 shows the evolution of the polar field (bottom), the tilt of the global dipole field (middle), and the maximum latitudinal extent of the heliospheric current sheet over a 14-year interval. The polar field panel, discussed above, shows the average of the line-of-sight fields observed in the north and south hemispheres - both 30-day averages and filtered 30-day averages. The dipole tilt angle is computed from WSO synoptic chart magnetic fields with the addition of the sharply peaked polar field described above. Data computed for each 10° in Carrington latitude are shown together with a 1-year low pass filter of the same data. During most of the solar cycle the magnetic dipole is nearly aligned with the Sun's rotation axis. There is a clear relation between the strength of the polar field and the dipole angle (and indeed they are not completely independent). When the polar field is weak, e.g. 1979 - 1984, there is more variability in the dipole tilt angle. The variability is caused by changes in the polar field strength and by variations in the equatorial dipole due to organization of active region fields after solar maximum. The maximum latitude of the heliospheric current sheet is derived from a model of the coronal field computed using a potential field model and the same photospheric field data. It, too, includes the sharply-peaked field derived from the polar observations. (Hoeksema, 1984, 1990). While the Earth never goes more than 7.25° from the solar equator, spacecraft and cosmic rays do. The intensity of cosmic rays is influenced by the direction of the interplanetary magnetic field (IMF) and by the latitudinal extent of the current sheet. Coronal observations and high latitude satellite observations are also consistent with the predicted current sheet latitude.

The Zonal Solar Magnetic Field

Another aspect of the global field is the axisymmetric or zonal magnetic field. The most familiar component of the zonal field is the total flux, shown in the bottom panel of Figure 3. The vertical axis contains data between $\sin(\Theta) = \pm 0.97$, corresponding to the center of the last aperture at 75°. The total flux is closely related to the level of activity and shows, much like the butterfly diagram of sunspot locations, how the eruption of flux progresses through the solar cycle. For this calculation the absolute value of the flux at each latitude was averaged for each Carrington Rotation. At the solar minima in 1976 and 1986 the total flux at all latitudes was low. About a year after minimum the level rose at mid-latitudes and rapidly expanded. The peak flux latitude gradually moved toward the equator in each hemisphere. The polar boundary of the shaded region (1 Gauss) never reached to very high latitude (perhaps in part because the measurements are not corrected for projection). The polar flux is strongest near solar minimum and decreases greatly at the time of polar reversal and for a couple years thereafter. The pattern of flux is fairly symmetric about the equator.

Not so familiar is the evolution of the net flux at each latitude versus time, shown in the next panel. In this case the signed field values are averaged for each rotation. This shows the axisymmetric contribution to the global field. Again, at minimum the net flux is fairly weak. The shading of different polarities (positive polarity is darker) shows that the axisymmetric flux is divided at the equator - like a dipole field. As the cycle progresses, two intensifying bands of opposite polarity emerge in each hemisphere, corresponding to the active regions. Following polarity (e.g. negative in the north in 1978) collects at higher latitude than preceding polarity. The preceding polarity intensifies toward maximum, but does not change latitude very much. The following polarity regions gradually extend toward the poles, reaching them in each hemisphere at, or a little after, solar maximum. There are some interesting features in 1980 and 1981 that appear to move poleward more rapidly and even cause brief reversals of the polar field direction. During the declining phase, the preceding polarity regions gradually decay until a simple dipolar configuration emerges again at minimum. The process begins again with the new cycle in 1986, which is remarkably similar to the previous cycle. The polar fields are very strong during the declining phase, at minimum, and during the first part of the rising phase.

The Sun's magnetic field is basically antisymmetric about the equator. The polar fields have opposite polarity and reverse at about the same time, active regions emerge with opposite polarity in the two hemispheres, and so on. So it is interesting to break the axisymmetric field into the two components that are symmetric and antisymmetric about the equator. The top panel in Figure 3 shows the dominant antisymmetric components of the zonal net flux. As expected, the polar fields and decaying active region fields show through very clearly. The mid-latitude boundary between the leading and following polarity zones is extremely flat until mid-1981 and never exceeds 30° (sine latitude = 0.5). The polar fields are very strong from 1983 through 1988 and appear to reverse cleanly in mid-1980 (obviously both are the same in the perfectly antisymmetric calculation). The features that move rapidly toward the poles are largely absent. There is a marginal suggestion of continuity between the leading polarity region of Cycle 21 (shaded in the north) that doesn't quite decay in 1985 and 1986 and the following polarity region of Cycle 22 that emerges in 1987. However the actual values are very near zero and may be falsely accentuated by the shading.

The symmetric part of the axisymmetric global field has some surprising features. The upper middle panel of Figure 3 shows very little strong field. The most interesting features are the three successive rapidly moving streams of alternating polarity that travel from the equator to the pole beginning in late 1979, mid 1980, and early 1981. They appear to reach the poles in about two years, which would correspond to a speed at the surface of about 30 m/s. The first stream feature is positive: it can be identified in the lower middle panel as the source of the brief relapse to positive polarity in the north in early 1981 and with the intensification of the southern field at the same time. The second feature appears at the equator in 1980 with negative polaiity and moves toward the poles at the same rate as the first. Its effects are seen in the intensification of the northern negative polar field in mid-1982, and in the apparent reversal of the southern field. Its influence can be seen in the total flux map in the lower panel as well. These first two features have almost no counterpart in the antisymmetric part of the flux. The third stream has positive polarity and does not reach all the way to the pole. There is a counterpart in the antisymmetric part. A polarity structure appearing in only one hemisphere produces a signal in both the symmetric and antisymmetric part. The third stream is much stronger in the southern hemisphere. The origin of these features is unknown, but may provide some clue to understanding how flux emerges in the solar cycle. The arrival of each of these streams can be seen in the polar field strength shown in Figures 1 and 2. In Cycle 22 the origins of positive and negative streams may be visible beginning in late 1989 and early 1990. There are only a few other intervals of strong

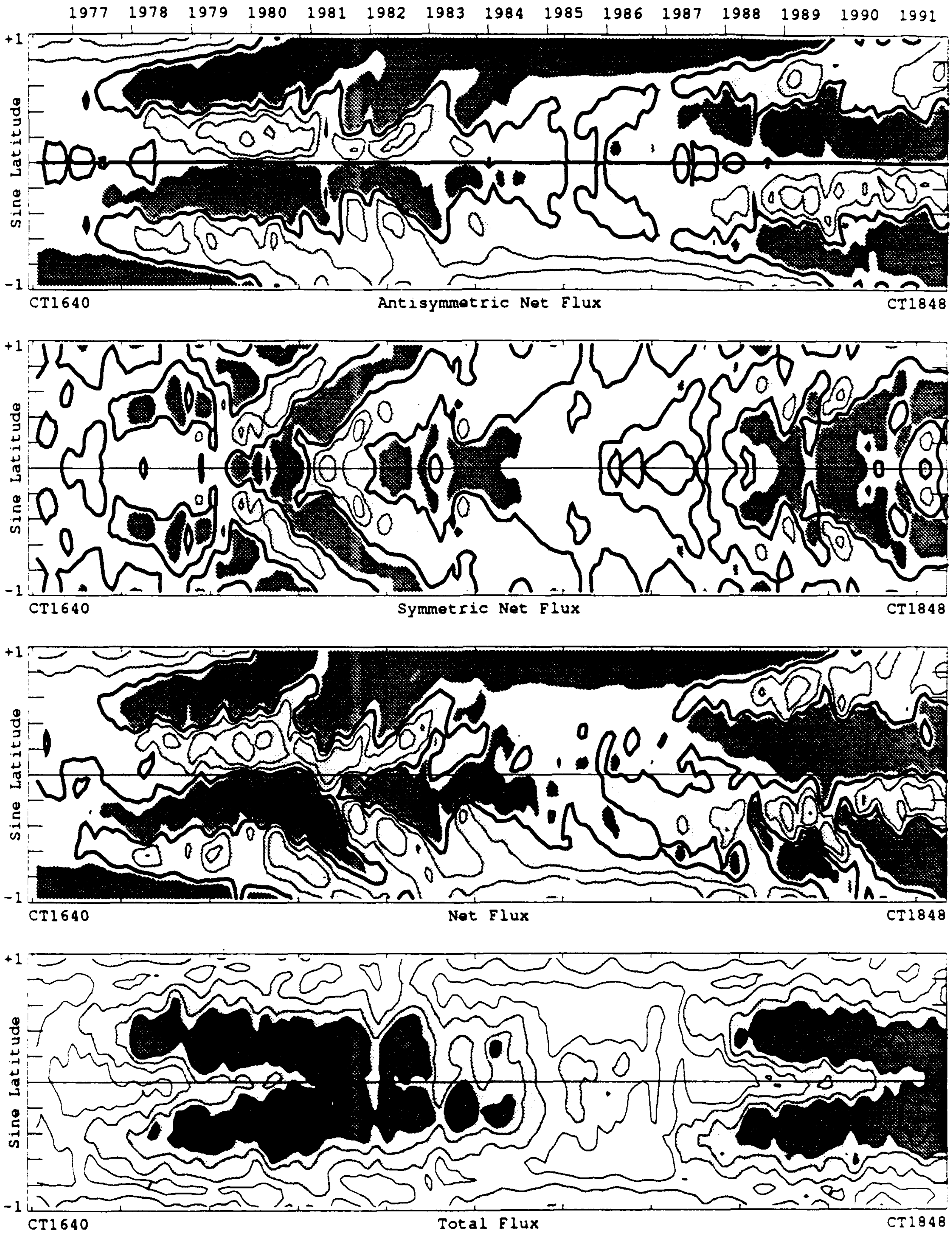
1977 1978 1979 1980 1981 1982 1983 1984 1985 1986 1987 1988 1989 1990 1991
+1
Sine Latitude
-1
CT1640
Antisymmetric Net Flux
CT1848
+1
Sine Latitude
-1
CT1640
Symmetric Net Flux
CT1848
+1
Sine Latitude
-1
CT1640
Net Flux
CT1848
+1
Sine Latitude
-1
CT1640
Total Flux
CT1848

symmetric flux, particularly in the early part of the cycle at mid latitudes, but most have counterparts in the antisymmetric flux and lie within the active region bands. They are probably due to imbalance in active region flux between the northern and southern hemispheres.

It is interesting to see if the same kinds of features are present in other solar cycles. There is evidence in Mt. Wilson data for similar rapidly poleward moving streams in Cycles 20 and 21 (Howard and LaBonte, 1981). Using Hα and prominence observations, Makarov and Sivaraman (1989a,b) have analyzed a great deal of data to reconstruct zonal polarity maps back to 1870. In most cycles, the polarity of one pole reversed more than once (only in the north after 1920, only in the south before). In each case of a multiple reversal, streams appeared near the equator and rapidly moved toward the poles in the corresponding hemisphere. Because only polarity information is available, it is not possible to see if the structures were present in both hemispheres, but it does not seem unlikely. If these fast symmetric poleward streams are present in most cycles, they may provide another clue for understanding how the solar cycle works.

The Rotation of the Solar Field

The rotation of the sun measured using Doppler shifts is well known (Scherrer et al., 1980; Howard et al., 1983). The rotation of the magnetic field patterns are less unambiguous. Snodgrass (1983) found that by correlating Mt. Wilson observations of individual magnetic features obtained over a few days, the Doppler rotation curve is found. Over longer intervals and on larger size scales the results are different. When correlating field patterns in Mt. Wilson and Kitt Peak magnetograms from one Carrington rotation with later rotations, a much broader, flatter, rotation curve is found (Stenflo, 1989). This is attributed to the difference in depth beneath the photosphere of the sources of the two patterns. Individual features presumably extend only a short distance below the photosphere and move with the photospheric gas, whereas the longer-lived, larger-scale patterns rotate with the source magnetic field pattern at the base of the convection zone. The source of the large-scale field must be deep because the rate of flux emergence implies that the large-scale pattern must be continually renewed on a relatively short time scale compared with a solar rotation.

Figure 3 : *(opposite page)* The lowest panel shows the evolution total flux versus sine of latitude and time as computed from WSO synoptic charts. For each latitude bin the average of the absolute values of the flux for each Carrington Rotation was computed and a contour plot made of the result. Contours are drawn at at 0.5, 1, 2, and 3 Gauss. Flux above 1 Gauss is shaded. The tick marks show 20 Carrington Rotation intervals. Years are shown at the top of the figure. The total flux is low near minimum in 1976. Flux emerges at relatively high latitude beginning in 1977. As maximum approaches, the latitude of maximum flux gradually decreases and the total flux present increases. The level and latitude decrease through the declining phase of the cycle and reach a minimum again in 1986. The appearance of the next cycle is very similar to Cycle 21. The polar flux is strongest at solar minimum. Notice the annual wave particularly obvious in the north. The next panel shows the net flux versus sine latitude and time. It is computed by adding up the flux for each latitude. Contours are at 0, ±0.5, 1, 2, and 3 Gauss. Positive field regions are shaded. The polar fields dominate at solar minimum. Opposite polarity flux zones emerge very soon after the total flux begins to increase. The latitudinal progression of the field is generally slow. There are some exceptions in 1980 - 1982. The field is mostly dipolar near minimum. Again, Cycles 21 and 22 are similar. The top two panels show the symmetric (second from the top) and antisymmetric (top) parts of the net flux relative to the equator. The contour levels and shading are the same. The polar fields and most of the cycle-related features dominate the antisymmetric top panel. The only strong features in the symmetric flux panel are associated with the rapidly moving features that move toward the poles from low latitudes after solar maximum.

This points out an important concern about the above-mentioned flux distribution model (DeVore and Sheeley,1987), which assumes a long lifetime (essentially infinite, unless annihilated) for flux elements emerging in active regions. Zirin (1987) points out that the recirculation of flux in the photosphere is immense. Globally, the flux emerging in small intranetwork fields is 100 times greater than the flux emerging in ephemeral regions and 10,000 times greater than the flux emerging in active regions. One would expect this flux to rapidly destroy any photospheric field pattern, though the flux is balanced on very small spatial scales and may simply increase the effective diffusion coefficient. It is also difficult to keep flux in the convection zone from being expelled because of buoyancy. If flux emerging in active regions really goes to the poles and waits to be destroyed at the following solar maximum, this requires an extremely stable anchor for the field. Yet if the flux is anchored deep within the Sun, how can the evolution of the field patterns be determined by the differential rotation, meridional flow, and diffusion observed in the photosphere? Stenflo also suggests that the flux distribution model cannot reproduce the two rotation curves on different time scales, but this seems erroneous. Sheeley and DeVore (1986) discussed how stationary 28- and 29-day recurrent patterns were likely to arise at higher latitudes from small elements moving with the photospheric gas, given the observed distribution of flux emergence.

These 28- and 29-day periods can be observed directly in the global field. Fourier analysis of long time strings of lower-resolution data from WSO shows that the large-scale field pattern rotates at different rates in the northern and southern hemispheres during Cycle 21: 28 days in the south and 26.9 days in the north (Antonucci et al., 1990). The computed coronal field shows the same disparity between the north and south in both Fourier analysis and autocorrelation, although the 28-day periodicity emerges in the south only after autocorrelation lags of six or more rotations (Hoeksema and Scherrer, 1987). At shorter lags the differential rotation is very broad, much like the curve for coronal holes. In the interplanetary medium the rotation is sampled only near the ecliptic, where two recurrence periods appear - again 28 days and 27 days (Svalgaard and Wilcox, 1975). These periods have been seen in IMF measurements over nearly 3 cycles, and in polarity determinations inferred from geomagnetic activity for the last 6 solar cycles. The coronal and photospheric results described above suggest that at least during Cycle 21 the two periods came from different solar hemispheres, the 27-day structure from the north and the 28-day from the south.

Summary and Conclusions

Several interesting aspects of the global field have been discussed. The polar fields reverse similarly in the two hemispheres. The field intensity differs from cycle to cycle and between the northern and southern hemispheres. While the reversal of the two is coordinated, the reversals do not occur simultaneously. The reversals appear to be the result of following polarity active region flux that makes its way to the poles.

This is shown more clearly in the zonal average net flux. Field emerging in active latitudes moves poleward. While most of the flux distribution is antisymmetric about the equator, several interesting symmetric streams of alternating polarity made their way rapidly from the equator to the pole during the last cycle. Upon reaching the pole they either reinforced or diminished the existing polar cap fields. Not all of these features occur in both hemispheres, but there is evidence that similar events have taken place in most solar cycles since at least 1870.

Solar rotation provides another way to look at the global field. While on the small scale the field rotates with the photospheric gas, on the large scale and over longer intervals the rotation is less differential. This may point to a deep source for the large-scale long-lived field, or to a particular distribution of flux emergence. In the corona it may simply be that, as the field complexity decreases with height, the differential rotation simplifies as well. It may be simplest to understand for the coronal field where, conceptually, the higher multipole components of the field decay most rapidly with height and thus the differential curve must become less steep. Similar simplification or averaging may explain the changes in rotation curve of the long-lived or large-scale fields. The asymmetry in rotation period between the northern and southern large-scale field patterns may explain the periods seen in the IMF for many years.

The global magnetic field must ultimately be explained in terms of the small-scale fields that compose it. Models that reproduce many of the general characteristics of the global field from observed active region emergence and known solar motions already exist. Unfortunately, this makes the explanation of the global field and the solar cycle more difficult! For instead of using the observable fields to explain the cycle, we must use the indirect information of when and where small-scale flux emerges. On the other hand, even the problem of flux distribution is unsolved, since it is difficult to explain the lifetimes of global patterns, considering the lifetimes of the flux elements. We may have to look to the base of the convection zone even to understand small-scale flux distribution in the photosphere.

Acknowledgements:

This work was supported in part by the Atmospheric Sciences Division of the National Science Foundation under Grant ATM 86-18263, by the Office of Naval Research under Contract N00014-89-J-1024, and by the National Aeronautics and Space Administration under Grant NGR 05-020-559.

References

Antonucci, E., J.T. Hoeksema, and P.H. Scherrer, Rotation of the Photospheric Magnetic Fields: A North-South Asymmetry, Astrophys. J., 360, 296, 1990.

Babcock, H., Astro. Phys. J., 130, 364, 1959.

DeVore, C., N. Sheeley, Jr., Simulations of the Sun's Polar Magnetic Fields During Sunspot Cycle 21, Solar Phys. 108, 47-59, 1987.

Duvall, T.L., Jr., A Study of Large-scale Solar Magnetic and Velocity Fields, Ph.D. Thesis, Stanford University, 1977.

Hoeksema, J.T., Structure and Evolution of the Large Scale Solar and Heliospheric Magnetic Fields, Ph.D. dissertation, Stanford University, 1984.

Hoeksema, J.T., and P.H. Scherrer, Rotation of the Coronal Magnetic Field, Astrophys. J. 318, 428, 1987.

Hoeksema, J.T., Large-scale Solar and Heliospheric Magnetic Fields, Adv. Space Res., in press, 1990.

Howard, R., and LaBonte, B.J., Solar Phys. 74, 131, 1981.

Howard, R., J.M. Adkins, J.E. Boyden, T.A. Cragg, T.S. Gregory, B.J. LaBonte, S.P. Padilla and L. Webster, Solar Rotation Results at Mount Wilson, Solar Phys. 83, 321-338, 1983.

Makarov, V.I., K.R. Sivaraman, Evolution of Latitude Zonal Structure of the Large-scale Magnetic Field in Solar Cycles, Solar Phys. 119, 35-44, 1989a.

Makarov, V.I., K.R. Sivaraman, New Results Concerning the Global Solar Cycle, Solar Phys. 123, 367-380, 1989b.

Scherrer, P.H., J.M. Wilcox, L. Svalgaard, T.L. Duvall, Jr., P.H. Dittmer, and E.K. Gustafson, The Mean Magnetic Field of the Sun: Observations at Stanford, Solar Phys., 54, 353-361, 1977.

Scherrer, P.H., J.M. Wilcox, and L. Svalgaard, The Rotation of the Sun: Observations at Stanford, Astrophys. J. 241, 811-819, 1980.

Sheeley, N.R., Jr., and C.R. DeVore, The Origin of the 28- to 29-Day Recurrent Patterns of the Solar Magnetic Field, Solar Phys. 104, 425-429, 1986.

Sheeley, N.R., Jr., Y.-M. Wang, and C.R. DeVore, Implications of a Strongly Peaked Polar Magnetic Field, Solar Phys. 124, 1-13, 1989.

Snodgrass, H.B., Magnetic Rotation of the Solar Photosphere, Astrophys. J. 270, 288-299, 1983.

Stenflo, J.O., Differential Rotation of the Sun's Magnetic Field Pattern, Astron. Astrophys. 210, 403-409, 1989.

Svalgaard, L., and J.M. Wilcox, Long Term Evolution of Solar Sector Structure, Solar Phys. 41, 461-475, 1975.

Svalgaard, L., T.L. Duvall, Jr., and P.H. Scherrer, The Strength of the Sun's Polar Fields, Solar Phys., 58, 225-240, 1978.

Tang, F. and H. Wang, Polar Fields During the Rising Phase of Cycle 22, Solar Phys., 132,247-256, 1991.

Zirin, H., Weak Solar Fields and Their Connection to the Solar Cycle, Solar Phys. 110, 101-107, 1987.